

## ***Original***

Jebril, S.; Mishra, Y.K.; Elbahri, M.; Kienle, L.; Greve, H.; Quandt, E.;  
Adelung, R.:

**Using thin film stress for nanoscaled sensors**

In: Materials Science Forum, THERMEC 2009 (2010) Trans Tech Publications

DOI: [10.4028/www.scientific.net/MSF.638-642.2028](https://doi.org/10.4028/www.scientific.net/MSF.638-642.2028)

## Using thin film stress for nanoscaled sensors

Seid Jebril, Yogendra K. Mishra, Mady Elbahri, Lorenz Kienle, Henry Greve,  
Eckhard Quandt, and Rainer Adelung<sup>a</sup>

Institute for Materials Science, CAU Kiel, Kaiserstr. 2, D-24143 Kiel

<sup>a</sup>ra@tf.uni-kiel.de

**Keywords:** Thin film, stress, nanowire, sensor

**Abstract.** Thin film stress is often seen as an unwanted effect in micro- and nanostructures. Since recent years, we could employ thin film stress as a useful tool to create nanowires. By creating stress at predetermined breaking points, e.g., in microstructured photo resist thin films, cracks occur on the nanoscale in a well defined and reproducible manner [1]. By using those as a simple mask for thin film deposition, nanowires can be created. More recently this fabrication scheme could be improved by utilizing delamination of the thin film, in order to obtain suitable shadow masks for thin film deposition in vacuum [2]. Now, these stress based nanowires can be integrated in microelectronic devices and used as field effect transistors or as hydrogen sensors [3]. For the functional part of the sensor, it was proposed that thin film stress created by hydrogen adsorption in the nanowire is the driving force. In terms of function, thin films can be also applied on free standing nanoscale whiskers or wires to modify their mechanical features or adding additional functionality. As a second example for the utilization of thin film stress, recent experiments on a piezoelectric and magnetostrictive material combination will be presented. These piezoelectric-magnetostrictive nano-composites are potential candidates for novel magnetic field sensors [4]. In these composites the magnetostriction will be transferred to the piezoelectric component, resulting in a polarization of the piezoelectric material, that can be used as the sensor signal. The results of two different composite layouts will be presented and discussed with a special focus on the comparison between classical macroscopic composites and the novel nanocomposites.

### Introduction

Stress determines the appearance and the functionality of thin films. Often stress evolves during the growth, if thin films are created by deposition, e.g., by physical vapor deposition (PVD) or chemical vapor deposition (CVD). A reason for that could be a deposition at elevated temperatures. This will lead to stress after cooling due to different thermal expansion coefficients. Even without temperature, stress evolves during growth. This is simply because the first layer of a freshly formed interface possesses a different equilibrium inter atomic distance due to a lower coordination compared to the bulk. A higher coordination appears after further growth. [5]. For thin film growth, several growth modes occur that follow basic rules [6]. In Volmer-Weber (VW) growth, the adatom-adatom interaction is stronger than the interaction of the adatoms with the surface, leading to the formation of three-dimensional adatom hills or islands. Growth of these clusters, along with coarsening, will cause rough multi-layer films to grow on the substrate surface. In contrast, in Frank-van der Merwe (FM) growth, adatoms attach preferentially to surface sites resulting in atomically smooth, fully formed layers. The stress resulting from both growth modes is different. This is not only an effect of epitaxial growth, even metallic glasses can exhibit these different growth modes that are coupled with a different thin film stress. Thin amorphous films of metallic glasses often develop intrinsic stresses during growth that can reach even GPa values [7]. In contrast to crystal systems, the amorphous thin films possess no long range structural order. Without any crystal anisotropy, systems do not allow typical crystal relaxation mechanisms, such as dislocation creep, which makes them the ideal model system for film growth concerning surface morphology and film stresses, independent of the details of the substrate for sufficient film thicknesses.[8]

The film accommodates the stress by inelastic and elastic deformations. The stress results in thin film tension, which can cause problems as the stress is often relaxed in an inelastic manner by buckling, cracking, bending or delamination. But even if the stress is relaxed elastically, the thin film properties and even sometimes the substrate properties (if the substrate is thin itself or relatively soft) are effected.

But there are also positive examples that utilize stress as a tool. Since 2004, thin film fracture was discovered as a structuring tool to fabricate nanowires [1,9]. Till today, more and more work was done to improve the first approach [10,11,12]. Recently, we showed that thin film stress relaxation can be used to create nanoscopic channels in photoresist that can be used as a template for nanowire formation in microchips to apply them as hydrogen sensors [3]. The underlying operation principle of the hydrogen sensor itself is also proposed to be a result of stress relaxation [13]. In a granular nanowire, consisting of a chain of Pd particles, the current flow is mainly limited by the interparticle boundary distance. Pd has the ability to take up large quantities of hydrogen, which is dissolved in the crystal lattice. Due to the additional volume, the Pd is exposed to stress, resulting in a relaxation by swelling of the Pd particles. This should diminish the distance between the particles and therefore increase the current through the granular nanowire.

A second example for the importance of stress can be found in a completely different type of sensor. In this, a combination of a magnetostrictive material and a piezoelectric material is employed to form a magneto-electric sensor. Applying a magnetic field to this system, the magnetostrictive material will expand. This creates stress that is coupled via the interface between the materials into the piezoelectric material resulting in a piezoelectric voltage. The interface has a very important role in order to transfer the elongation. A second important role of the interface is its influence on the stress development in the material during growth for the device. Often, a piezoelectric crystal is used as substrate, subsequently magnetostrictive material is grown on top. As described above, this can lead itself to large interfacial stresses, that might influence the coupling of the materials.

## Experimental

In general, the fabrication of the nanowire within the fracture approach microchips contains 5 steps, compare [3]. First, a photoresist, Shipley 1813, is deposited on a silicon samples by spin coating as a thin film of ~560 nm thickness. This turns out to be an optimal thickness to induce fracture. Too thin films do not create enough stress for cracking, too thick films develop too much stress leading to complete delamination. In a second step, photolithography is used to microstructure the photoresist. The lithography was done on silicon substrates (76 mm-diameter, p-doped, 1-10  $\Omega$  cm resistivity, 380  $\mu$ m thick, <100> oriented and terminated with a 100 nm thick thermally grown SiO<sub>2</sub>). Third, the samples are exposed to a thermal cycling down to cryogenic temperatures in order to induce the stress in the photoresist thin film that relaxes inelastically to nanoscopic fracture patterns in the microstructured photoresist thin film. The cracks were induced after baking the microstructured resist at a temperature about 360 K for 30 minutes. The already baked sample was quenched to an extremely cold bath of liquid nitrogen which has a temperature about 77 K. Stripes of photoresist with a width of 10 micrometer and a length of 200  $\mu$ m create a well defined 'zig zag' pattern of cracks. The fourth step contains the deposition of metals by a PVD-process. In this step of the process, metal deposition was done at ultrahigh vacuum (UHV) at a base pressure of 10<sup>-8</sup> mbar. This deposition of metal covers the whole area including the cracks. About 50 nm thick metals layers of Au Pd and Ti were deposited for the corresponding nanowire formation, before a thin layer of Ti or Cr was used as adhesion promoter. The fifth final step is to separate the superfluous metal from the microstructured contacts resulting in nanosized wires formed within the surface cracks. This photoresist mask lift off was performed by first soaking the sample in acetone for about 1 minute and then keeping it in an ultrasonic bath for roughly 2 seconds. Keeping the sample for long time in an ultrasonic bath may destroy the nanowires.

For the second example FeCoBSi is deposited on ZnO. ZnO is grown by a modified Vapor Liquid Solid process [14]. The experimental setup consists of a chemical vapor transport tube furnace. ZnO micro particles were dispersed on a silicon substrate and mixed with graphite powder in a ceramic crucible. The tube furnace has different temperature zones allowing evaporation and condensation of the Zn.

FeCoBSi was subsequently sputtered on the ZnO crystals by RF sputtering in a Von Ardenne CS 730 S sputter system. The base pressure of the chamber is  $10^{-8}$  mbar, during deposition the Argon gas pressure was kept at  $6 \cdot 10^{-3}$  mbar. The applied RF power was 500 W which yields in a deposition rate of 0.11 nm/s.

The samples were characterized by using different analytical techniques. A Park Autoprobe atomic force microscope was used to study the grainy nature (surface topography) of the fabricated nanowires. A Phillips XL 30 scanning electron microscope was used to analyze the surface structure and geometry of both the delaminated film and nanowires. It is also equipped with an EDAX EDX detector for detail analysis of the chemical composition. The hydrogen sensor test is done by using a chamber in which a controlled gas atmosphere can be created. The current was measured by a Keithley picoammeter in a simple custom made vacuum chamber.

For a detailed TEM investigation, the ZnO nanostructures were analyzed by high resolution transmission electron microscopy (HRTEM) with a Philips CM 30ST microscope (LaB<sub>6</sub> cathode, 300 kV, C<sub>s</sub> = 1.15 mm). HRTEM micrographs (multislice formalism) were simulated with the EMS program package (spread of defocus: 70 Å, illumination semi-angle: 1.2 mrad). All images were evaluated (including Fourier filtering) with the programs Digital Micrograph 3.6.1 (Gatan) or Crisp (Calidris). Chemical analyses by EDX were performed with a Si/Li detector (Noran, Vantage System).

## Results and discussion

The procedure described in the experimental chapter in order to form the stress induced nanostructures is applied to form a hydrogen wire based on Palladium as described in the introduction. Fig. 1 shows the typical result of a fabrication process. Fig. 1a illustrates the layout of the microchip, which basically contains "blocked" contact lines between different contact pads. The magnification shows a 3 dimensional setup where the nanowires will be formed. Two openings are intersected by a 10 μm wide stripe of photoresist. After inducing the thermal stress, the stripe is fractured in a zig-zag pattern, Fig. 1b shows a scanning electron microscopy image (width of the stripe is 10 micrometer). After metal deposition and lift off processes, the cracks are converted to nanowires. The microstructured openings are now converted to micro contact lines leading to the contact pads, see SEM image in Fig. 1c. The AFM image in figure 1d shows an approximately 40 nm wide wire.

Such wires exhibit a granular structure. In this setup, a hydrogen sensor can be build by using Pd wires. The current-voltage behavior of the wires is shown in fig. 2. Exposure to hydrogen will typically shift the current voltage curve by reducing drastically the resistance, as shown in fig. 2a. Two mechanisms can occur at hydrogen exposure of the Pd nanowire; the hydrogen adsorption can result in the diffusion of hydrogen into the grains (clusters) which can increase the resistance of the nanowire by creating additional electrons scattering centers. On the other hand, the formation of PdH<sub>x</sub> phase results in stress that relaxes, as there are no constraints, as an expansion of the palladium lattice in the grains. This can lead to an increase in conductivity of the nanowires by decreasing the inter grain gap distance. Since the overall conductivity is the superposition of these two effects, it depends on the setup of the wire which one is dominating. Wires that do not show many gaps tend to result in an electrical conductivity decrease as shown in Fig 1b. The reverse effect can also be observed upon removing the hydrogen.

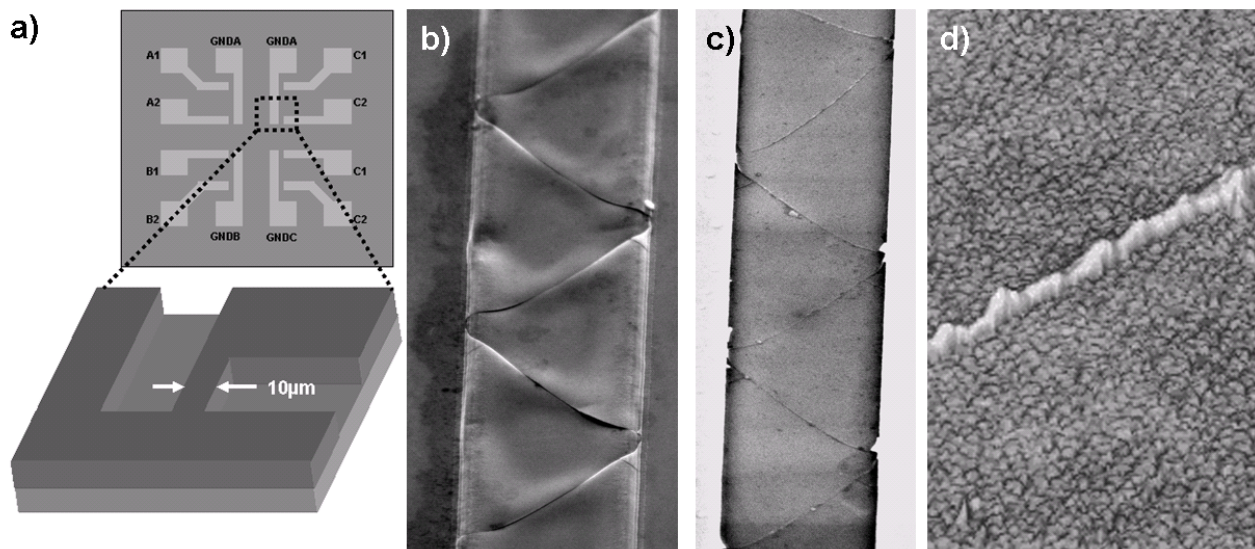


Fig. 1 Setup of a nanowire device fabricated by thin film stress induced fracture a) Layout of the microchip b) SEM image showing the 10  $\mu\text{m}$  wide photo resist strip after relaxing the stress in a zig-zag shaped fracture pattern. c) Metallization and photoresist masked lift off leads to a zig-zag nanowire pattern between metal contacts. d) 3D representation of an AFM scan of a 40 nm wide nanowire.

The nanoscale hydrogen sensors can be very fast in reaction, no matter in which direction it is changing the resistance, as it can be seen in fig. 2c. Within parts of seconds, a small amount of hydrogen (10%) will be detected. The whole setup is reproducible, the resistance changes for different microchips fabricated in the same manner is around 20%. For comparison, also gold and anodized Ti nanowires were fabricated in a similar manner. While the gold nanowires show some change to hydrogen (but only about one quarter compared with Pd), the anodized Ti nanowires did not show any change in resistivity. The detailed results on this comparison will be published elsewhere after further measurements.

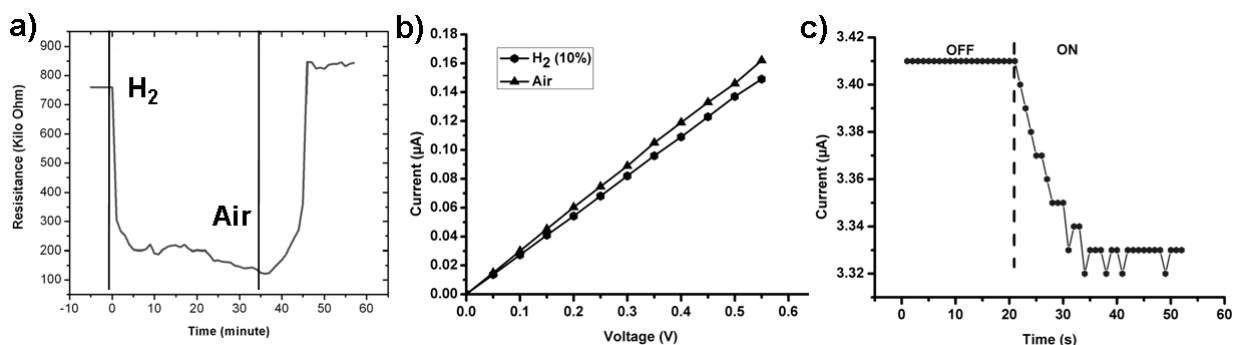


Figure 2. Electrical measurements on the change of current after hydrogen exposure. a) A gap controlled nanowire sensor shows a decrease in resistance b) Pd-nanowires with a weak resistance increase upon hydrogen exposure. c) Fast response time of the nanowire sensor.

Figure 3 gives a second example where thin film stress can be used to control the morphology of a sensor. As explained in the introduction, the interface between a piezoelectric material and a magnetostrictive is highly important for the stress induced strain transfer between the two functional layers. Also here, nanoscopically different surfaces induce a varied thin film growth, resulting in different stress states. Fig 2a shows a high magnification of a needle shaped ZnO crystal examined by TEM (Transmission electron microscopy). The thin film is single crystalline beside a small layer of  $\sim 2.5$  nm on the surface. ZnO crystals fabricated in conventional CVD by using gold as precursor and do not show an amorphous top layer. After the deposition of the FeCoBSi different growth

modes can be observed, even so both of the deposited thin films are almost perfectly amorphous. On the conventional grown samples, the thin film appears extremely smooth with no visible surface roughness, see fig 3b, compare with [15]. In contrast, fig. 3c shows the film on top of the ZnO needle, which is visibly rough and appears like grown in the VW growth mode. Fig. 3d is a magnification, revealing the crystalline to amorphous boundary. The local roughness equals the whole film thickness. The images show that the appearance of the roughness of the thin film does not depend on the orientation of the crystalline facets. Control experiments with gold crystals and ZnO structures grown by a conventional vapor liquid solid process [15] show in any orientation no roughening of the deposited thin film, neither on the gold nor on the ZnO surface.

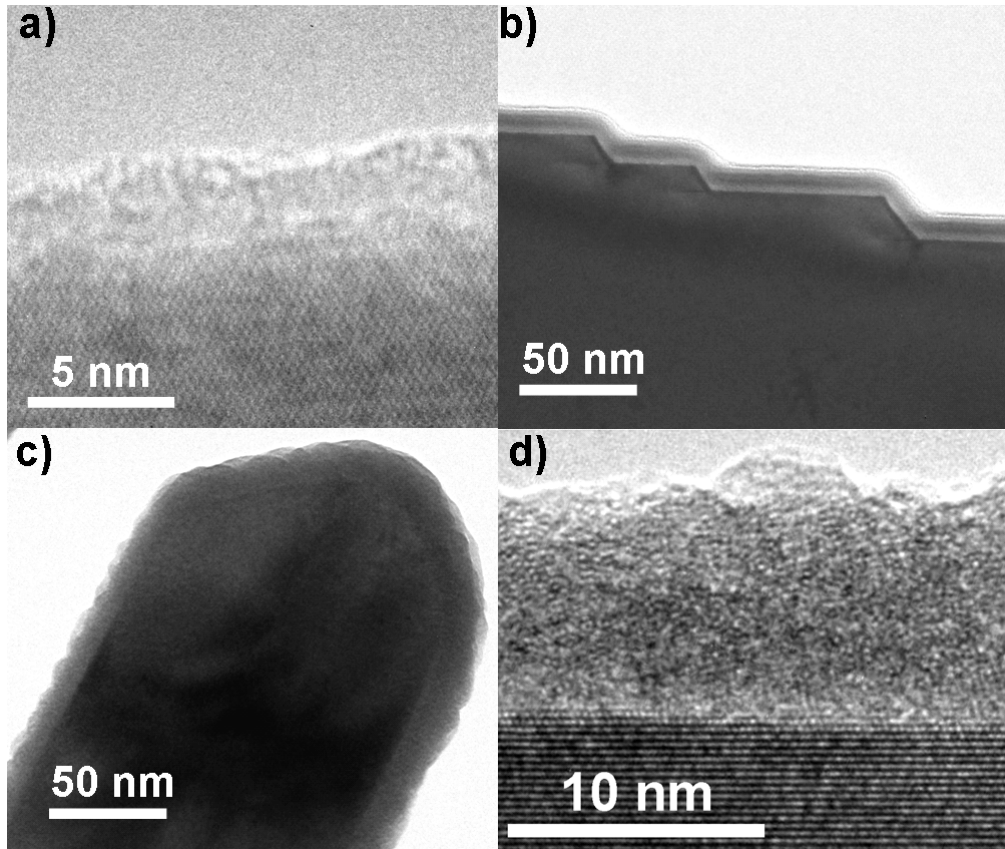


Figure 3. ZnO, covered with different materials. a) ZnO crystal showing an amorphous surface layer b) ZnO crystal covered by a smooth FeCoBSi- thin film c) ZnO crystal covered by a rough FeCoBSi thin film d) magnification of c, showing the crystalline ZnO (bottom) to amorphous FeCoBSi-boundary.

A model explanation for the intrinsic stress formation in amorphous thin film growth can be given by Mayr and Samwer [8]. In this publication an independence of the morphology and stresses of the details of various substrates was found, except for the very early stages of film growth, similar to what is observed in figure 3c, where different orientations give a similar surface roughness. The authors suggests nondiffusional energy minimizing mechanisms at the surface to the generation of film stresses: A surface diffusion on the metallic glass is unlikely, as the control experiments with smooth interfaces show almost no roughening on the surface. This rules out stress-induced surface modification by externally applied or lattice-mismatch-driven film stresses for crystalline solids, which are based on directed diffusion from the valleys to the hills in the surface structures due to stress-induced changes in local chemical potentials like in the Asaro-Tiller-Grinfeld instability [16], as explained in [8]. In the amorphous systems like in metallic glasses where many energetically equivalent, mainly randomly distributed positions exist on its surface, misfit energy is typically negligible. Assuming a very low adatom mobility, a modified adatom

density is propagated into the interior of the film, that leads to a typically compressive biaxial film stress based on the difference of surface stress and surface energy. But a three dimensional, hill forming growth generates tensile stresses due to local energy minimization by viscous coalescence in a dynamic equilibrium of stress generation and surface energy reduction. Thus, at one certain thickness of a rough metallic glass thin film can be found at which the tensile and compressive stress states cancel each other, and the film is stress free on a global perspective. In the system of Mayr and Samwer, this is the case at a thickness of ~300 nm. In comparison to the control experiments, which leads to flat surfaces, a creation of a stress free film is not possible until a surface roughening will be observed. Here, the rough structures may originate from island growth on top of a substrate in early stages of growth. By tuning the initial surface roughness, a variation of the ideal, stress free thin film thickness should be possible.

### Conclusion

The experiments above show some examples for the utilization of stress in sensors. In contrast to the first guess, stress is not necessarily an unwanted effect. It can be used for the creation of sensors as it is illustrated by the thin film fracture approach. It is the underlying principle of operation for a Pd hydrogen sensor and the coupled piezoelectric-magnetostrictive sensor. Furthermore, it can be used as an optimization tool in the magnetostrictive component of such sensors, it can be employed for the design of the magneto-electric sensors that are composed of a piezoelectric and a magnetostrictive component.

### Acknowledgement

We gratefully acknowledge support by the German Science Foundation (DFG), Project AD 183/4-3 the Heisenberg Professorships (AD 183/5-1, KI 1263/2-1) and the authors would like to thank Prof. Dr. Dr. h.c. mult. A. Simon for enabling and V. Duppel for performing the TEM study.

### References

- [1] R. Adelung, O.C. Aktas, J. Franc, A. Biswas, R. Kunz, M. Elbahri, J. Kanzow, U. Schürmann and F. Faupel, *Nature Mat.* 3, 375, (2004).
- [2] M. Elbahri, S. K. Rudra, S. Wille, S. Jebril, M. Scharnberg, D. Paretkar, R. Kunz, H. Rui, A. Biswas and R. Adelung, *Adv. Mater.* 18, 1059 (2006).
- [3] S. Jebril, M. Elbahri, G. Titazu, K. Subannajui, S. Essa, F. Niebelschütz, C.-C. Röhlig, V. Cimalla, O. Ambacher, B. Schmidt, D. Kabiraj, D. Avasti and R. Adelung, *Small* 4, 2214, (2008).
- [4] E. Quandt, S. Stein and M. Wuttig, *IEEE Trans. Mag.* 41, 3667 (2005).
- [5] A. G. Evans and J. W. Hutchinson, *Acta Metall. Mater.* 43, 2507 (1995).
- [6] Oura, K.; V.G. Lifshits, A.A. Saranin, A.V. Zotov, and M. Katayama in: *Surface Science: An Introduction*. Berlin: Springer (2003).
- [7] M. Moske and K. Samwer, *Z. Phys. B* 77, 3 (1989).
- [8] S. G. Mayr and K. Samwer, *Phys. Rev. Lett.* 87, 036105, (2001).
- [9] B. E. Alaca, H. Sehitoglu, and T. Saif, *Appl. Phys. Lett.* 84, 4669 (2004).
- [10] D. Salac and W. Lu, *Comp. Mater. Sci.* 39, 849 (2007).
- [11] D. Salac and W. Lu, *Nanotech.* 17, 5185 (2006).
- [12] O. Sardan, A.D. Yalcinkaya, and B.E. Alaca, *Nanotech.* 17, 2227 (2006).
- [13] F. Favier, E. Walter, M.P. Zach, T. Benter and R.M. Penner, *Science*, 293, 2227 (2001).
- [14] X. Wen, Y. Fang, Q. Pang, C. Yang, J. Wang, W. Ge, K. S. Wong and S. Yang, *J. Phys. Chem. B* 109, 15303 (2005).
- [15] L. Kienle, V. Duppel, R. Adelung, E. Quandt, S. Müller, C. Ronning and A. Simon. *Z. Kristallogr. Suppl.* 27 (2009), in press.
- [16] R. J. Asaro and W. A. Tiller, *Metall. Trans. A* 3, 1789 (1972)